

Properties of thin strained Ga(As,P) layers

M.-E. Pistol, M. R. Leys, and L. Samuelson

Department of Solid State Physics, University of Lund, P.O. Box 118, S-221 00 Lund, Sweden

(Received 24 August 1987)

In this paper we present results of studies on samples, grown by metal-organic vapor-phase epitaxy, containing a single layer of Ga(As,P) in between GaP. Investigations of these samples were carried out by means of photoluminescence at 2 K and the results are confronted with calculations using deformation-potential theory. It is shown that strain effects decrease the band-gap energy of the layers and that good agreement can be obtained between theory and experiment. Finally, we discuss quantum size shifts and increased phonon coupling which occur for thin wells ($< 100 \text{ \AA}$).

I. INTRODUCTION

It is possible to grow perfect epitaxial structures containing layers with nonequal lattice constants, e.g., in the systems GaAs-GaP and GaAs-InAs. Such structures then contain layers with elastically strained crystal lattices. This strain will affect the band structure of the material, allowing the fabrication of materials in which the band gap and the lattice constant are independently variable.¹ The ability to fabricate such "strained" epitaxial layers thus offers extra flexibility in materials science. In this paper, we first describe the growth, by metal-organic vapor-phase epitaxy (MOVPE), of thin (down to four atomic layers) strained layers of Ga(As,P) in between GaP and show the photoluminescence spectra of these layers. In the third section we present the principles of deformation-potential theory and show how strain effects alter the energy of the electron-hole recombinations in the Ga(As,P) layers. Then, we discuss the band offsets in the GaP/Ga(As,P)/GaP system. Also, we calculate here quantum size effects and discuss the increased phonon coupling which is observed in the thinner ($< 100 \text{ \AA}$) layers.

II. EXPERIMENT

Double heterostructures of GaP/Ga(As,P)/GaP were grown by metal-organic vapor-phase epitaxy (MOVPE) in a horizontal reactor operating at atmospheric pressure. As starting compounds, trimethyl gallium (TMGa), phosphine, (PH_3 , pure), and arsine (AsH_3 , 5% in hydrogen) were used. The various components were introduced into the reactor by means of pneumatically operated valves fitted with a purge line through which a hydrogen flow was continuously passed. The substrates were gallium phosphide, sulfur-doped to $\approx 5 \times 10^{17} \text{ cm}^{-3}$ and with orientation $(100) \pm 0.5^\circ$. The etch pit density of these substrates was $\approx 10^5 \text{ cm}^{-2}$. Directly on these substrates, a $5\text{-}\mu\text{m}$ -thick layer of GaP was grown with a high growth rate ($5 \mu\text{m/h}$) and at a high temperature (775°C). The actual region of interest [the GaP/Ga(As,P)/GaP structure] was grown at a temperature of 715°C and with a lower TMGa partial pressure so that a growth rate of 1

monolayer per second could be maintained throughout. The PH_3 -to-TMGa ratio was kept at a value of about 16 for both these growth rates. In preliminary experiments, it has been found that under the above-mentioned conditions morphologically smooth GaP layers could be grown having a residual n -type impurity concentration of $\leq 5 \times 10^{15} \text{ cm}^{-3}$.

To grow the Ga(As,P) layers, AsH_3 was introduced into the reactor for a fixed period of time; the growth (TMGa introduction) was not interrupted at the interfaces. The thinnest Ga(As,P) layers were made to a thickness of 11 \AA and grown in 4 s. The thickest Ga(As,P) layers grown were $0.13 \mu\text{m}$. The top GaP layer was typically 800 \AA . Micrographs of cross sectional images made by transmission electron microscopy showed that the change in composition in our epitaxial structures was achieved in one or two monolayers and that the interfaces were extremely flat. A micrograph of a $32\text{-}\text{\AA}$ -thick $\text{Ga}(\text{As}_{0.30}\text{P}_{0.70})$ layer in between GaP is shown in Fig. 1.

The AsH_3 concentrations introduced into the reactor were varied to give Ga(As,P) layers with various compositions. The concentration of arsenic in these layers was determined by SIMS measurements to an accuracy of about 10–15 relative percents. The maximum concentration of arsenic built into the Ga(As,P) layers was 48%.

When strained layers are grown thin enough, the misfit between epilayer and substrate can be completely accommodated by elastic deformation of the crystal lattice. The growth is then commensurate with perfect registration of lattice planes through the interfaces. Above a certain (so-called "critical") layer thickness the epilayer breaks up and misfit dislocations are formed. Based on an analysis of the forces exerted on threading dislocations (originating from the substrate) a model has been developed for the calculation of the critical layer thickness as function of the misfit between epilayer and substrate.² Thus, for $\text{Ga}(\text{As}_x\text{P}_{1-x})$ layers strained to the lattice parameter of GaP one obtains a critical layer thickness of about 400 \AA for $x = 0.1$ (0.4% misfit); the critical layer thickness is about 90 \AA with $x = 0.3$ (corresponding to 1.1% misfit), whereas for $x = 0.5$ (1.9% misfit) the critical layer thickness is approximately 25 \AA .

Photoluminescence studies were carried out on the

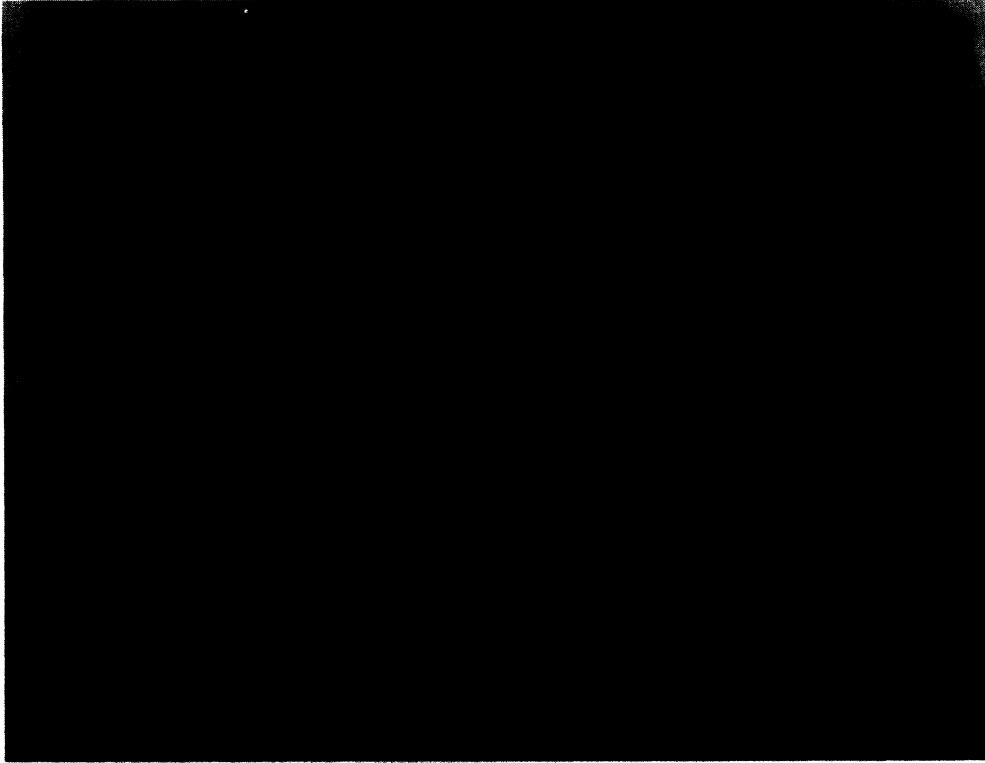


FIG. 1. Bright field micrograph of a 32-Å-thick Ga(As_{0.30}P_{0.70}) layer in between GaP, showing interface abruptness and flatness. No dislocations are present at the interfaces.

GaP/Ga(As,P)/GaP structures with the samples at 1.5 K and excited by the 351-nm line of an Ar⁺ laser. The excitation density was approximately 100 W/cm². In Fig. 2, photoluminescence (PL) spectra of thin strained layers of Ga(As_{0.30}P_{0.70}), having thicknesses of 120, 50, and 11 Å, are shown. The shape of the PL peak of the strained Ga(As,P) layer is similar to that of the M_0^X peak in indirect, unstrained Ga(As,P), including the LA^X phonon replica at about 30 meV lower energy.³ In the case of relaxed indirect-gap Ga(As,P), the M_0^X peak is believed to be due to the recombination of electrons and holes which are trapped in the density of states (DOS) tail that extends into the forbidden gap. The width of the peak is then related to the energy distribution of the disorder-induced DOS tail and amounts to about 7 meV. The line width of the PL peak of the 120-Å sample is also about 7 meV. From the similar line shape and width we conclude that we observe the same PL transition. The peak maximum of the 120-Å, strained Ga(As,P) layer lies at 2.015 eV. The peak maximum of a thick, relaxed Ga(As,P) layer of this composition lies at 2.17 eV. The observed energy shift of 150 meV is due to the compressive strain exerted on the Ga(As,P) layer.

In Fig. 3, we show data obtained from PL measurements on samples with varying Ga(As,P) layer thicknesses and with various compositions of the ternary layer. For the Ga(As_{0.12}P_{0.88}) layers, the strain gives rise to an energy shift of approximately 50 meV. For the Ga(As_{0.48}P_{0.52}) layers the measured band-gap energies are

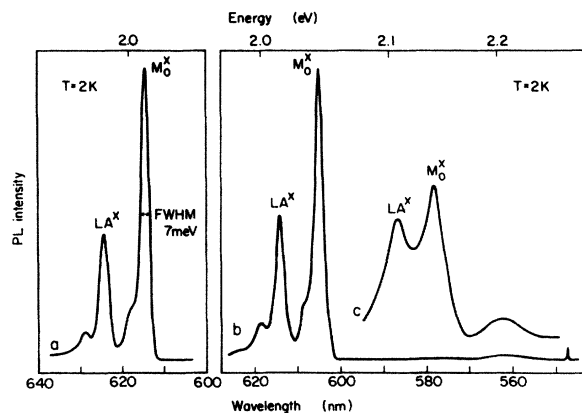


FIG. 2. 2-K photoluminescence of strained, 120, 50-, and 11-Å-thick Ga(As_{0.30}P_{0.70}) layers (curves a, b, and c, respectively) in between GaP. The peak maximum for the 120-Å layer is at 2.015 eV, the peak width is 7 meV. The luminescence intensity is very strong compared to the GaP band-edge emission around 2.2 eV. As the layers get progressively thinner the ratio of the LA^X phonon-assisted transition to the no-phonon transition increases. The energy difference between the PL peak energy between the 120-Å layer and the 50-Å layer is about 30 meV, and is attributed to quantum size effects. The increased phonon coupling for the 50-Å layer is believed to be due to quantum size effects on the Γ band (not seen in PL) which is discussed in the text.

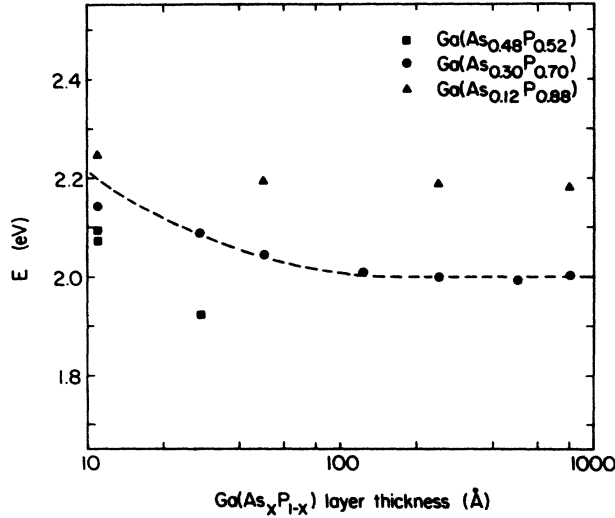


FIG. 3. The transition energies for quantum wells of three different compositions as a function of the quantum well width. Points are included for layers thicker than the critical layer thickness. For narrow well widths the transition energies increase; shown in the figure with a dashed line is the calculated energy shift as a function of quantum well width for $\text{Ga}(\text{As}_{0.30}\text{P}_{0.70})$.

strongly dependent on the layer thickness. In this series of samples containing extremely thin layers with high arsenic concentration, small variations in the growth rate and AsH_3 flow rate give rise to large variations of the PL peak position. In these samples grown to the same intended thickness and arsenic concentration, variations of up to 100 meV in the PL peak position were observed. In the other sets of samples one observes an increase in the measured luminescence energy for layer thicknesses below 100 Å. At these thicknesses, quantum size effects will start to increase the transition energies.

The result of a finite quantum-well calculation for a single quantum well in the $\text{GaP}/\text{Ga}(\text{As}_{0.30}\text{P}_{0.70})/\text{GaP}$ system (as carried out in, e.g., Ref. 4) is also shown in the figure. This calculation will be discussed in the next section. Furthermore, from Fig. 3 one may observe that strain-shifted photoluminescence is obtained even from layers grown to thicknesses above the calculated critical thickness. Thus, the PL peak was still intense in $\text{Ga}(\text{As}_{0.12}\text{P}_{0.88})$ layers of 800 and 1300 Å (not included in the figure). In the $\text{Ga}(\text{As}_{0.30}\text{P}_{0.70})$ layers, the strain-related PL peak is still present in layers up to 800 Å thick. In this series of samples, a decrease in PL peak intensity was observed when the ternary layer thickness exceeded 500 Å (i.e., about 5 times the critical thickness). In the series of the $\text{Ga}(\text{As}_{0.48}\text{P}_{0.52})$ samples, strain-related PL was observed for 50-Å layers (about two times the critical thickness); in this case, however, the intensity was low and the peak was extremely broad.

III. THEORY

In the structures of $\text{GaP}/\text{Ga}(\text{As,P})/\text{GaP}$, the strain in the $\text{Ga}(\text{As,P})$ layer is compressive in the (100) plane and

tensional in the [001] direction. The shift of the energy levels due to strain effects can be calculated via deformation-potential theory, as described by, e.g., Mathieu *et al.*,⁵ in which orbital strain terms and strain-dependent spin-orbit terms are incorporated in the Hamiltonian.

First, we treat the calculation for the valence band where the relevant Hamiltonian is equal to

$$H = H_1 + H_2, \quad (1)$$

where H_1 contains the orbital strain terms and thus can be written as

$$\begin{aligned} H_1 = & -a_1(e_{xx} + e_{yy} + e_{zz}) \\ & -3b_1[(L_x^2 - \frac{1}{3}L^2)e_{xx} + \text{c.p.}] \\ & -\sqrt{3}d_1[(L_xL_y + L_yL_x)e_{xy} + \text{c.p.}], \end{aligned} \quad (2)$$

and H_2 contains the strain-dependent spin-orbit terms, as follows:

$$\begin{aligned} H_2 = & -a_2(e_{xx} + e_{yy} + e_{zz})\mathbf{L}\cdot\boldsymbol{\sigma} \\ & -3b_2[(L_x\sigma_x - \frac{1}{3}\mathbf{L}\cdot\boldsymbol{\sigma})e_{xx} + \text{c.p.}] \\ & -\sqrt{3}d_2[(L_x\sigma_y + L_y\sigma_x)e_{xy} + \text{c.p.}]. \end{aligned} \quad (3)$$

The terms \mathbf{L} and $\boldsymbol{\sigma}$ are the angular momentum operator and the Pauli spin matrix. The abbreviation c.p. stands for cyclic permutation. The terms a_1 , a_2 , b_1 , b_2 , d_1 , and d_2 are the experimentally determined deformation potentials. The strain tensor components are present as the terms e_{ij} . The stress-strain relation is contained in the stress-strain tensor and is expressed in the following matrix:

$$\begin{pmatrix} e_{xx} \\ e_{yy} \\ e_{zz} \end{pmatrix} = \begin{pmatrix} S_{11} & S_{12} & S_{12} \\ S_{12} & S_{11} & S_{12} \\ S_{12} & S_{12} & S_{11} \end{pmatrix} \begin{pmatrix} X_{xx} \\ X_{yy} \\ X_{zz} \end{pmatrix}, \quad (4)$$

where S_{ij} are the elastic compliances and X_{ii} are the stresses applied to the sample under consideration. For our calculations we used the compliances as given in Ref. 5: $S_{11} = 0.973 \times 10^{-6} \text{ bar}^{-1}$ and $S_{12} = -0.299 \times 10^{-6} \text{ bar}^{-1}$.

For compression in a (100) plane (normal to the z direction) one gets

$$e_{zz} = 2 \frac{S_{12}}{S_{12} + S_{11}} e_{xx}, \quad e_{xx} = e_{yy} = e. \quad (5)$$

Next, we treat the calculation for the conduction-band Hamiltonian. The Γ conduction-band Hamiltonian under strain is

$$H_\Gamma = C_1(e_{xx} + e_{yy} + e_{zz}) \quad (6)$$

whereas the X conduction-band Hamiltonian must be written as

$$\begin{aligned} H_X = & E_1(e_{xx} + e_{yy} + e_{zz}) \\ & + E_2\mathbf{n} \cdot [\mathbf{e} - \frac{1}{3}(e_{xx} + e_{yy} + e_{zz})\mathbf{1}] \cdot \mathbf{n}. \end{aligned} \quad (7)$$

In the above, C_1 , E_1 , and E_2 are deformation potentials, e is a unit 3×3 matrix, 1 the unit dyadic, and n is a unit vector in the $[100]$ directions.

Our subsequent treatment differs from that of Mathieu *et al.* in that we make no approximation in diagonalizing the valence-band Hamiltonian. This approximation leads to large deviations at the higher ($e > 1\%$) values of strain which are the values we have to consider in our materials system. Diagonalizing the Hamiltonians H_1 and H_2 and subtracting the valence-band eigenvalues from the conduction-band eigenvalues then results in the following expressions for the transition energies as a function of strain (e):

$$\begin{aligned}
 D'_1 &= A_0 + \frac{1}{2}(\Delta'_0 - B) - \frac{1}{2}[(\Delta'_0 + B)^2 + 8(B')^2]^{1/2}, \\
 D'_2 &= A_0 + B, \\
 D'_3 &= A_0 + \frac{1}{2}(\Delta'_0 - B) + \frac{1}{2}[(\Delta'_0 + B)^2 + 8(B')^2]^{1/2}, \\
 I'_1 &= A_X + \frac{2}{3}G + \frac{1}{2}(\Delta'_0 - B) - \frac{1}{2}[(\Delta'_0 + B)^2 + 8(B')^2]^{1/2}, \\
 I'_2 &= A_X + B + \frac{2}{3}G, \\
 I'_3 &= A_X - \frac{1}{3}G + \frac{1}{2}(\Delta'_0 - B) - \frac{1}{2}[(\Delta'_0 + B)^2 + 8(B')^2]^{1/2}, \\
 I'_4 &= A_X + B - \frac{1}{3}G, \\
 I'_5 &= A_X - \frac{1}{3}G + \frac{1}{2}(\Delta'_0 - B) + \frac{1}{2}[(\Delta'_0 + B)^2 + 8(B')^2]^{1/2},
 \end{aligned} \quad (8)$$

where constants from Ref. 5 are used:

$$\begin{aligned}
 A_0 &= -10.833e, \\
 A_x &= 3.057e, \\
 B &= 2.670e, \\
 G &= -13.384e, \\
 B' &= 3.487e, \\
 \Delta'_0 &= 0.09 - 6.76e + 1.336e.
 \end{aligned} \quad (9)$$

The term $6.76e$ in the expression for Δ'_0 takes into account the change in spin-orbit energy between GaP and GaAs.

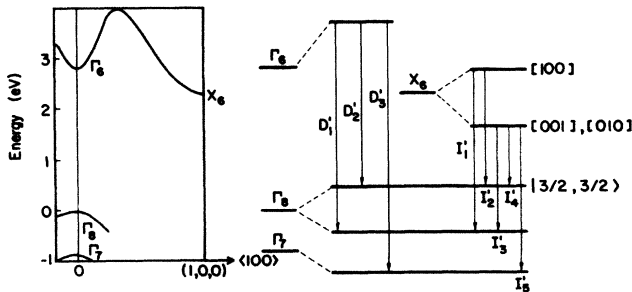


FIG. 4. A figure of the band structure of GaP and the shift of the energy levels in indirect Ga(As,P) as a result of compressional strain in the (100) plane and tensional strain in the $[100]$ direction, according to deformation-potential theory. The lines labeled by D'_1, D'_2, \dots are direct transitions and I'_1, I'_2, \dots are transitions from the different indirect conduction band valleys as illustrated. Their strain dependence is displayed in Fig. 5.

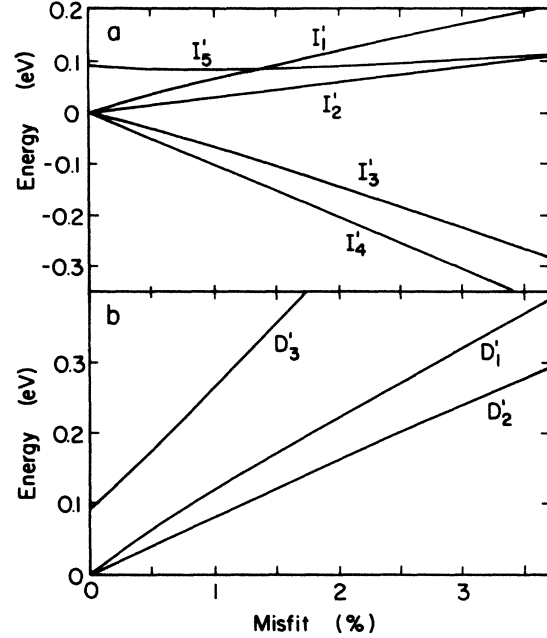


FIG. 5. (a) A plot of the calculated energy differences in Ga(As,P) as a function of misfit for the X minima. The notation is explained in Fig. 4. (b) The same plot as in (a), but in this case for the Γ minimum.

In Fig. 4 the band structure and the relevant transitions for indirect Ga(As,P) are shown. It can be seen that as a result of strain, the Γ level shifts upwards, whereas the X level splits with the $[100]$ and $[010]$ valleys going down in energy. In the valence band, the maximum splits into two states. Only the lowest-energy transition, I'_4 , is seen in photoluminescence. Quantitatively, the strain-induced energy change of I'_4 results in a linear decrease in energy with respect to M_0^x of about 10 meV per 0.1% misfit. In Fig. 5 the calculated energies as a function of misfit are shown.

IV. RESULTS AND DISCUSSION

In Fig. 6 the band-gap variations as function of x are shown for the bulk (relaxed) alloy,⁶ while, by the dotted line, the band-gap variation as a function of x is shown for the alloy, strained to the lattice constant of GaP. Experimental data obtained from the samples with various compositions are also included in this figure. There is good agreement between the calculation and the experimental data points. We stress the fact that in the calculations we have assumed that the relevant electron-hole transitions take place entirely in the strained Ga(As,P) layer with a transition from the lowest X minimum to the valence-band maximum. Also, the similar shape of the M_0^x peak in bulk Ga(As,P) and Ga(As,P) as a strained layer in between GaP favors an interpretation of an intrawell transition. This means that the strained Ga(As,P) provides a well for both electrons and holes. In Ref. 7 a model was proposed, based on photoluminescence mea-

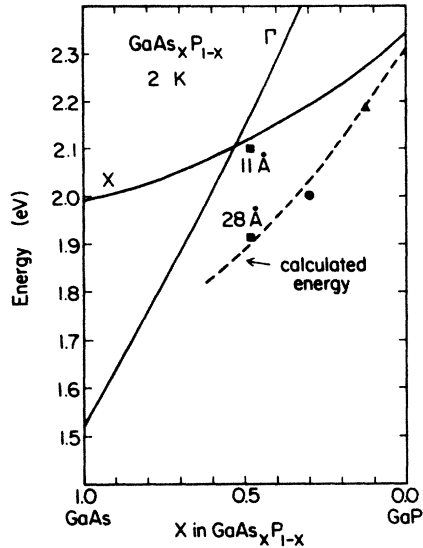


FIG. 6. Photoluminescence transition energies for quantum wells of different compositions. The solid line is the band gap of the unstrained alloy and the dashed line is the calculated band-gap shift due to strain. The offset is due to the binding energy of the M_0^X .

measurements at 77 K, that there is a staggered band offset in the Ga(As,P)/GaP system, with the conduction band being lowest in the GaP layers, while the valence-band level was highest in Ga(As,P). This type of structure will give rise to charge separation and interwell recombinations. We now propose a model as illustrated in Fig. 7 for the development of the band structure in the GaP/Ga(As,P)/GaP materials system. The first step is based upon the finding that in the alloy the resulting band-gap change occurs mostly in the valence band, with a slope of about 5 meV per percent arsenic.⁸ The second step in Fig. 7 is based upon the fact that application of

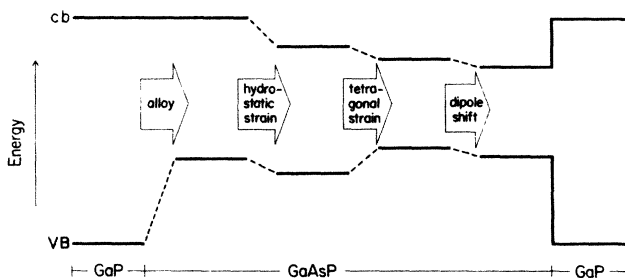


FIG. 7. An illustration of the band lineups. Unstrained Ga(As,P) has a valence band that increases with increasing As content which gives a lineup with GaP where the largest offset is in the valence band. The hydrostatic component of strain then mostly affects the conduction-band minimum. The tetragonal component of strain then further shifts the band edges as illustrated. Other effects such as dipole layers in the interface are expected to affect the final lineup, leaving uncertainty in the actual band offsets.

hydrostatic strain on Ga(As,P) results in a small shift in the valence band (with a deformation potential of +0.9 eV) and a larger (deformation potential of +1.4 eV) shift in the conduction band.⁹ The third step shows the effect of tetragonal strain, which decreases the conduction-band edge and increases the valence-band edge. In the final step, charge rearrangement is introduced which effectively lowers both band edges.

In Fig. 2 we show the 2-K luminescence spectra of three samples of Ga(As_{0.30}P_{0.70}) with thicknesses of, respectively, 120, 50, and 11 Å. The PL peak maxima are to be found at 2.015, 2.049, and 2.146 eV, respectively. The shapes of the PL peaks of all three samples are very similar but it is clear that there is an energy shift due to the already mentioned quantum effects. One can also observe that the intensity of the LA^X phonon replica is enhanced with respect to the M_0^X peak when the well thickness decreases. Furthermore, it is noted that the width of the PL peaks increases with decreasing layer thickness; thus, with a layer thickness of 50 Å the PL peak width is equal to 9 meV and for the 11-Å layer the peak width is approximately 15 meV. As this latter layer is only 4 atomic layers thick, it can be expected that the interface imperfections on the atomic scale start to play a role here. We will first discuss the quantum size effects and then the enhanced phonon coupling.

As already mentioned when discussing Fig. 3, a finite quantum-well calculation for a single quantum well in the GaP/Ga(As_{0.30}P_{0.70})/GaP system has been carried out. For this materials system electron masses and heavy-hole masses in Ga(As,P) of $0.6m_0$ and $0.3m_0$, respectively, were used¹⁰ and the potential steps in the conduction band and in the valence band were taken to be 0.10 and 0.17 eV, respectively. The result of this calculation is shown in Fig. 3 and serves to give a first check on the magnitude of the quantum size effects. Given the uncertainties in the band offsets it is noted that the quantum energy shift as calculated with the above-mentioned parameters follows the trend of the experimental data remarkably well. The difference between our system and that discussed in Ref. 7 is that in our case only the Ga(As,P) layer is strained, whereas in Ref. 7 the Ga(As,P)/GaP superlattice was grown on an epilayer of intermediate composition. In this case the strain is then shared between both Ga(As,P) (in compression) and GaP (in tension) and then slightly different values of the deformation potentials can make the GaP layer a well for electrons. We conclude that also in the Ga(As,P)/GaP system prestrain can be used as a means of changing superlattices from type I to type II, as has been established in the Si/SiGe system.¹¹

Now we discuss the enhanced phonon coupling which takes place in the thinner (<100 Å) strained layers. From Fig. 2 it can be seen that the intensity of the LA^X phonon replica line with respect to the M_0^X peak increases from a value of $\approx \frac{1}{3}$ for the 120-Å layer, via $\approx \frac{1}{2}$ for the 50-Å layer, up to a value of $\approx \frac{2}{3}$ for the thinnest Ga(As,P) layer.

Previous investigations of shallow donor-acceptor-pair spectra in GaP have shown that the phonon coupling of luminescent transitions in indirect GaP is dependent on

the degree of mixing of the direct, Γ -point wave function into the indirect X -point wave function.¹² Thus the wave function of the particular, luminescing state can be written as

$$\Psi = \alpha_X \phi_X + \alpha_\Gamma \phi_\Gamma, \quad (10)$$

where ϕ_X derives from the X point and ϕ_Γ derives from the Γ point. The factor α_X is approximately unity but the factor α_Γ , which determines the strength of the non-phonon transition, is a sensitive function of the band structure. In a first approximation one can write α_Γ as follows:

$$\alpha_\Gamma = V / (E_\Gamma - E_X), \quad (11)$$

where V is a constant and $E_\Gamma - E_X$ is the energy difference between the X point and the nearest Γ -point conduction-band minimum. This energy difference is affected by the layer thickness and increases for the thinner wells. As the electron has a lighter mass in the Γ -point state than in the X -point state one can expect a larger quantum size effect for the Γ -point state and thus an increase in $E_X - E_\Gamma$ for thin, quantum well layers. It is noted that even with a not-too-large staggered X -band offset the Ga(As,P) layer can act as a well for Γ electrons. The resulting decrease of α_Γ will decrease the nonphonon transition strength compared to the phonon-assisted transition and give rise to the relative increase of the LA^X transition, which is what is observed in the PL spectra of the samples shown in Fig. 2. We have previously shown³ that the variation in the M_0^X line shape (or phonon coupling) with alloy composition can be explained with a similar band-structure-dependent zero-phonon transition probability. This effect is also expected to occur in superlattices and is then one of the properties of the superlattice which can be adjusted independently of some other property; e.g., the band gap. As has been pointed out by Osbourn,¹ the ability to independently vary several properties of strained-layer superlattices is an important advantage of the strained materials systems as compared to the more limited flexibility of lattice-matched superlattices such as GaAs/AlGaAs.

V. CONCLUSIONS

We have made use of MOVPE to grow extremely thin strained layers of Ga(As,P) in a matrix of gallium phosphide. Extremely strong and narrow photoluminescence

peaks were obtained from the strained layers present in these samples. For layers with a thickness of 3–5 times the theoretical value of the critical layer thickness the PL due to the strained layer was still present. After that, the strain-related PL peak intensity gradually decreased. From this behavior we conclude that the strain in the layers is relieved only gradually. With layers grown above the critical thickness and after a crosshatch pattern is observable on the crystal surface, strained regions remain present in the crystal and can still give rise to the strain-related PL peak.

Calculations of the effect of strain on the band gap by means of deformation-potential theory showed that strain decreases the band-gap energy. Assuming only intrawell transitions within the Ga(As,P) layer the calculations and the experimental data points are in good agreement with each other and show that a strain-induced energy decrease of up to 170 meV has been obtained. In our samples the transition energies decrease by approximately 10 meV per 0.1% misfit. We propose a model for the development of the band structure in the GaP/Ga(As,P)/GaP system taking into account alloy effects, hydrostatic and tetragonal strain and interface effects. From a comparison with previous work¹ it is noted that prestrain changes this superlattice from type I to type II.

With layers thinner than 100 Å, quantum size effects occur which tend to increase the transition energy again. The observed quantum effects can be correlated to simple theory, again assuming that electron-hole transitions take place only inside the Ga(As,P) well.

Finally, we have observed an increase in the phonon coupling in structures with strained layers thinner than ≈ 100 Å. This has been explained in terms of a change in the degree of mixing of the direct Γ -point wave function into the indirect, X -point wave function, due to quantum size effect on the Γ -point wave function. This shows again the flexibility of the strained-layer materials systems.

ACKNOWLEDGMENTS

Special thanks to H. Titze for technical assistance with the crystal growth, to J. Petruzello from Philips Research laboratories, Briarcliff Manor, New York, for the TEM micrograph and to U. Södervall from Chalmers University, Gothenburg, Sweden, for the SIMS measurements. This work was supported by grants from the National Swedish Board for Technical Development and by the Swedish Natural Science Research Council.

¹G. C. Osbourn, *J. Vac. Sci. Technol. B* **1**, 379 (1983).

²J. W. Matthews, in *Epitaxial Growth* (Academic, New York, 1975), p. 559.

³L. Samuelson and M.-E. Pistol, *Solid State Commun.* **52**, 789 (1984).

⁴P. M. Frijlink and J. Maluenda, *Jpn. J. Appl. Phys.* **21**, L574 (1984).

⁵H. Mathieu, P. Merle, E. L. Ameziane, B. Archilla, J. Camassel, and G. Poiblaud, *Phys. Rev. B* **19**, 2209 (1979).

⁶D. J. Wolford, J. A. Bradley, K. Fry, J. Thompson, and H. E. King, in *Proceedings of the 13th International Symposium on GaAs and Related Compounds*, edited by G. E. Stillman (The Institute of Physics, London, 1982).

⁷P. L. Gourley and R. M. Biefeld, *J. Vac. Sci. Technol.* **21**, 473 (1982).

⁸L. Samuelson, M.-E. Pistol, and S. Nilsson, *Phys. Rev. B* **33**, 8776 (1986).

⁹L. Samuelson and S. Nilsson, *J. Lumin.* (to be published).

¹⁰*Physics of Group IV Elements and III-V Compounds*, Vol. 17, Part a of *Landolt-Börnstein, Numerical Data and Functional Relationships in Science and Technology*, edited by O. Madelung (Springer-Verlag, Berlin, 1982).

¹¹G. Abstreiter, H. Brugger, T. Wolf, H. Jorke, and H. J. Herzog, *Phys. Rev. Lett.* **54**, 2441 (1985).

¹²T. N. Morgan, *Phys. Rev. Lett.* **21**, 819 (1968).

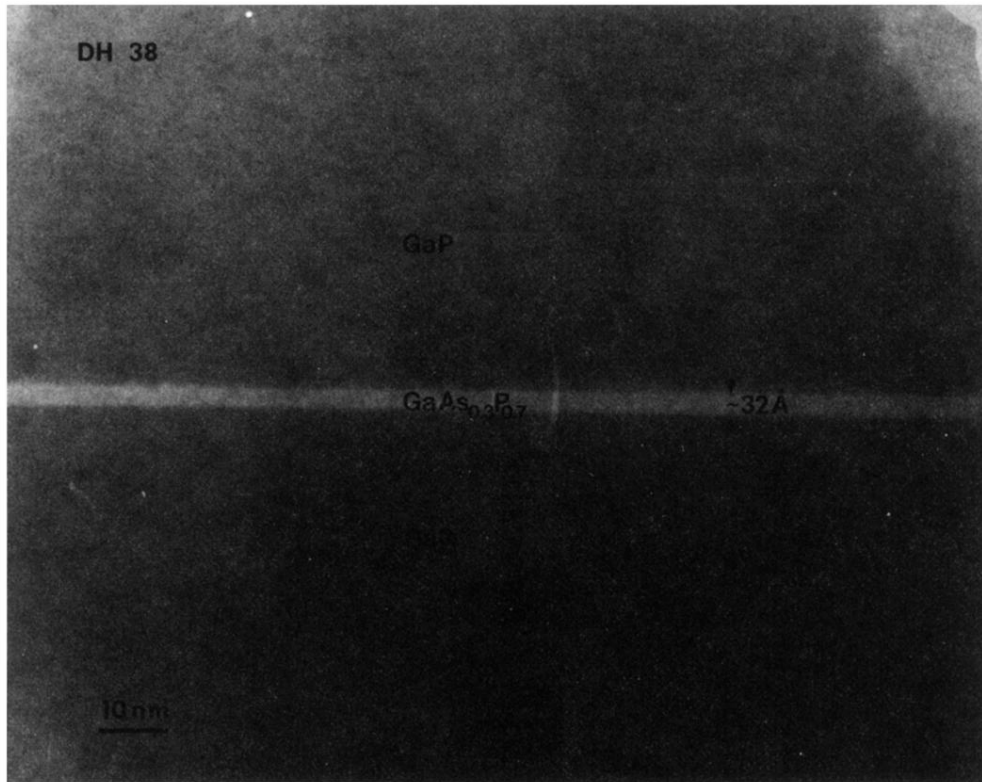


FIG. 1. Bright field micrograph of a 32-Å-thick $\text{Ga}(\text{As}_{0.30}\text{P}_{0.70})$ layer in between GaP, showing interface abruptness and flatness. No dislocations are present at the interfaces.